ELSEVIER

The Journal of Heart and Lung Transplantation

http://www.jhltonline.org

ORIGINAL PRE-CLINICAL SCIENCE

Epicardial infarct repair with bioinductive extracellular matrix promotes vasculogenesis and myocardial recovery

Holly E.M. Mewhort, MD,[a] Jeannine D. Turnbull, BSc,[a] Alessandro Satriano, PhD,[b] Kelvin Chow, PhD,[c] Jacqueline A. Flewitt, MSc,[b] Adin-Cristian Andrei, PhD,[d] David G. Guzzardi, BSc,[a] Daniyil A. Svystonyuk, BSc,[a] James A. White, MD, FRCSC,[b] and Paul W.M. Fedak, MD, PhD, FRCSC[a,d]

From the [a]Division of Cardiac Surgery; [b]Stephenson Cardiovascular MR Centre, Department of Cardiac Sciences, Libin Cardiovascular Institute of Alberta, University of Calgary, Calgary, Alberta, Canada; [c]Department of Biomedical Engineering, University of Alberta, Edmonton, Alberta, Canada; and the [d]Bluhm Cardiovascular Institute, Northwestern University, Chicago, Illinois.

KEYWORDS:
heart failure;
myocardial infarction;
extracellular matrix;
angiogenesis;
cardiac MRI;
ischemia-reperfusion

BACKGROUND: Infarcted myocardium can remodel after successful reperfusion, resulting in left ventricular dilation and heart failure. Epicardial infarct repair (EIR) using a bioinductive extracellular matrix (ECM) biomaterial is a novel surgical approach to promote endogenous myocardial repair and functional recovery after myocardial infarction. Using a pre-clinical porcine model of coronary ischemia-reperfusion, we assessed the effects of EIR on regional functional recovery, safety, and possible mechanisms of benefit.

METHODS: An ECM biomaterial (CorMatrix ECM) was applied to the epicardium after 75 minutes of coronary ischemia in a porcine model. Following ischemia-reperfusion injury, animals were randomly assigned in 2:1 fashion to EIR ($n = 8$) or sham treatment ($n = 4$). Serial cardiac magnetic resonance imaging was performed on normal ($n = 4$) and study animals at baseline (1 week) and 6 weeks after treatment. Myocardial function and tissue characteristics were assessed.

RESULTS: Functional myocardial recovery was significantly increased by EIR compared with sham treatment (change in regional myocardial contraction at 6 weeks, 28.6 ± 14.0% vs 4.2 ± 13.5% wall thickening, $p < 0.05$). Animals receiving EIR had reduced adhesions compared with animals receiving sham treatment (1.44 ± 0.51 vs 3.08 ± 0.89, $p < 0.05$). Myocardial fibrosis was not increased, and EIR did not cause myocardial constriction, as left ventricular compliance by passive pressure distention at matched volumes was similar between groups (13.9 ± 4.0 mm Hg in EIR group vs 16.0 ± 5.2 mm Hg in sham group, $p = 0.61$). Animals receiving EIR showed evidence of vasculogenesis in the region of functional recovery.

CONCLUSIONS: In addition to the beneficial effects of successful reperfusion, EIR using a bioinductive ECM enhances myocardial repair and functional recovery. Clinical translation of EIR early after myocardial infarction as an adjunct to surgical revascularization may be warranted in the future.

J Heart Lung Transplant 2016;35:661–670

Reprint requests: Paul W.M. Fedak, MD, PhD, FRCSC, C880, 1403-29 Street NW, Calgary, Alberta T2N 2T9, Canada. Telephone: +403-944-5931. Fax: +403-270-3715.

E-mail address: paul.fedak@gmail.com

Advances in the management of myocardial infarction (MI) have improved survival after MI. However, the incidence of ischemic heart failure is increasing.[1] Coronary

1053-2498/$ - see front matter
http://dx.doi.org/10.1016/j.healun.2016.01.012

artery bypass grafting (CABG) is sometimes performed early after MI, but complete revascularization is not always achieved, and CABG does not directly target the infarcted myocardium. Myocardial remodeling can result in interstitial fibrosis, progressive ventricular dilation, and subsequent heart failure. "Biosurgical" strategies applied at the time of surgical revascularization specifically to target the infarcted myocardium may help promote healing, prevent heart failure, and improve outcomes for patients with preexisting ischemic injury.

The extracellular matrix (ECM) influences cardiac remodeling and function after MI. Healthy ECM provides structural support to tissues and regulates cardiac cell morphology, differentiation, migration, and proliferation,[2] which act in concert to impact tissue function. After tissue injury, ECM is essential for endogenous repair and may mediate the potential for cellular regeneration.[3,4] The application of a biologic ECM construct with bioinductive properties from retained growth factors, cytokines, and matricellular proteins, such as porcine small intestine submucosa extracellular matrix (SIS-ECM), may enhance endogenous tissue repair. SIS-ECM is a decellularized ECM construct that retains its native three-dimensional architecture and cell signaling proteins, providing a homeostatic environment to promote cell function and survival.[5–7] CorMatrix ECM (CorMatrix Cardiovascular, Inc., Roswell, GA) is a commercially available SIS-ECM that is approved by the US Food and Drug Administration and has been used previously in cardiac surgery applications.[8–17]

We established proof-of-concept for epicardial infarct repair (EIR) with SIS-ECM in a rodent model demonstrating that local application of SIS-ECM biomaterial to the epicardial surface of infarcted myocardium limits structural remodeling after MI and improves myocardial function.[8] The epicardium itself is a key player in repair after MI. Following ischemia, endogenous cells within the epicardium become activated, resulting in epicardial thickening.[18] This process mobilizes key progenitor cell niches located within the epicardial space by epithelial mesenchymal transition (EMT).[19–22] Epicardial progenitor cells differentiate into (myo)fibroblasts, vascular smooth muscle cells, or cardiac myocytes.[19,20,22] Restoring local homeostatic queues by application of a healthy biologic ECM construct containing angiogenic growth factors may enhance differentiation toward a vascular phenotype, promoting endogenous healing pathways beneficial in the setting of ischemia.

In this study, we examined the influence of EIR using SIS-ECM on regional myocardial recovery as an adjunct to successful reperfusion after MI. We assessed procedural safety, efficacy on regional functional recovery, and possible mechanisms of post-MI repair for EIR.

Methods

Experimental animals

All animal experiments were performed in accordance with the Canadian Council on Animal Care Guide for the Care and Use of Experimental Animals and the National Society for Medical Research Guide for the Care and Use of Laboratory Animals and approved by the University of Calgary Animal Care Committee. Male Landrace pigs weighing 25 kg were obtained from Neufeld Farms (Alberta, Canada).

Ischemia-reperfusion model and EIR procedure

The ischemia-reperfusion model was adapted from the Gorman Cardiovascular Research Group sheep model.[23] Animals were intubated and mechanically ventilated with medical-grade oxygen and 2% to 3% isoflurane and administered continuous infusions of lactated Ringer's solution (0.04 ml/kg/min) and lidocaine (0.04 mg/kg/min). After median sternotomy, diagonal branches of the left anterior descending coronary artery were ligated for 75 minutes and then reperfused. Animals were then randomly assigned 2:1 to receive EIR or a sham procedure. Animals receiving EIR received SIS-ECM (CorMatrix-ECM) secured to the epicardial surface of the heart overlying the infarct territory using a running 5-0 polypropylene (Prolene) suture. Animals receiving sham treatment received a running 5-0 Prolene suture encompassing the infarct border without securing SIS-ECM.

Cardiac magnetic resonance image acquisition

Serial cardiac magnetic resonance (CMR) imaging was performed at baseline (1 week) and 6 weeks after treatment. Animals were mechanically ventilated, and anesthesia consisting of inhaled isoflurane ($\leq$1.0%) and nitrous oxide ($\leq$1.0%) and a continuous intravenous infusion of ketamine (0.3 mg/ml), fentanyl (0.04 mg/ml), and midazolam (0.025 mg/ml) at a rate of 30 to 100 ml/hour was maintained to achieve a mean arterial pressure $>$60 mm Hg. CMR imaging was performed using a 1.5-tesla magnetic resonance imaging scanner (Avanto; Siemens Healthcare GmbH; Erlangen, Germany) at the Stephenson Cardiac MR Center (Calgary, Alberta, Canada). Images were acquired using cine imaging, late gadolinium enhancement (LGE), and T1-mapping by saturation recovery single-shot acquisition[24] protocols.

CMR image analysis

CMR images were analyzed by readers blinded to treatment group using cvi 42 software (Circle Cardiovascular Imaging, Inc., Calgary, Alberta, Canada). The left ventricle was divided into a 3 $\times$ 24-segment model, and infarcted myocardium was defined as all segments with $>$50% LGE at a threshold of $>$5 SD above the mean. The peri-infarct zone was defined as all segments immediately adjacent to any infarcted segment. All remaining segments were defined as remote to the infarct territory.

Regional myocardial function was measured as an average of the percent wall thickening of all segments within a defined territory. Myocardial fibrosis was quantified by measuring the mean extracellular volume (ECV) within a defined territory calculated from regional pre-contrast and post-contrast T1 values. Mean peak systolic strains stratified by territory were measured using a custom-built multi-axial adaptation of the algorithm described by Satriano et al.[26] A clinical cardiologist (J.A.W.) with expertise in CMR imaging blinded to treatment group reviewed all analyses.

Post-mortem assessment

After final CMR imaging, animals were euthanized with intravenous saturated potassium chloride (20 ml) under full anesthesia.

An anterolateral thoracotomy was performed, and the dissection of intrathoracic adhesions between the posterior sternal surface and the pericardium (Figure 1A) was evaluated by 3 independent observers, blinded to the treatment group, using an adapted semi-quantitative scale (Table 1).[27,28] Adhesion tenacity was graded according to the extent of blunt vs sharp dissection required. Hearts were explanted and sectioned in short axis. Transmural biopsy specimens of the infarct, peri-infarct, and remote myocardial territories were taken.

Histology

Myocardial biopsy specimens were fixed in 10% Neutral Buffered Formalin (VWR International, Inc., West Chester, PA), embedded in paraffin, and stained with Masson's trichrome. Vascular densities were quantified by averaging the number of vascular structures per high-power field in 3 randomly captured images of the infarcted myocardium per animal. Images were reviewed and interpretations confirmed by a clinical pathologist blinded to treatment group.

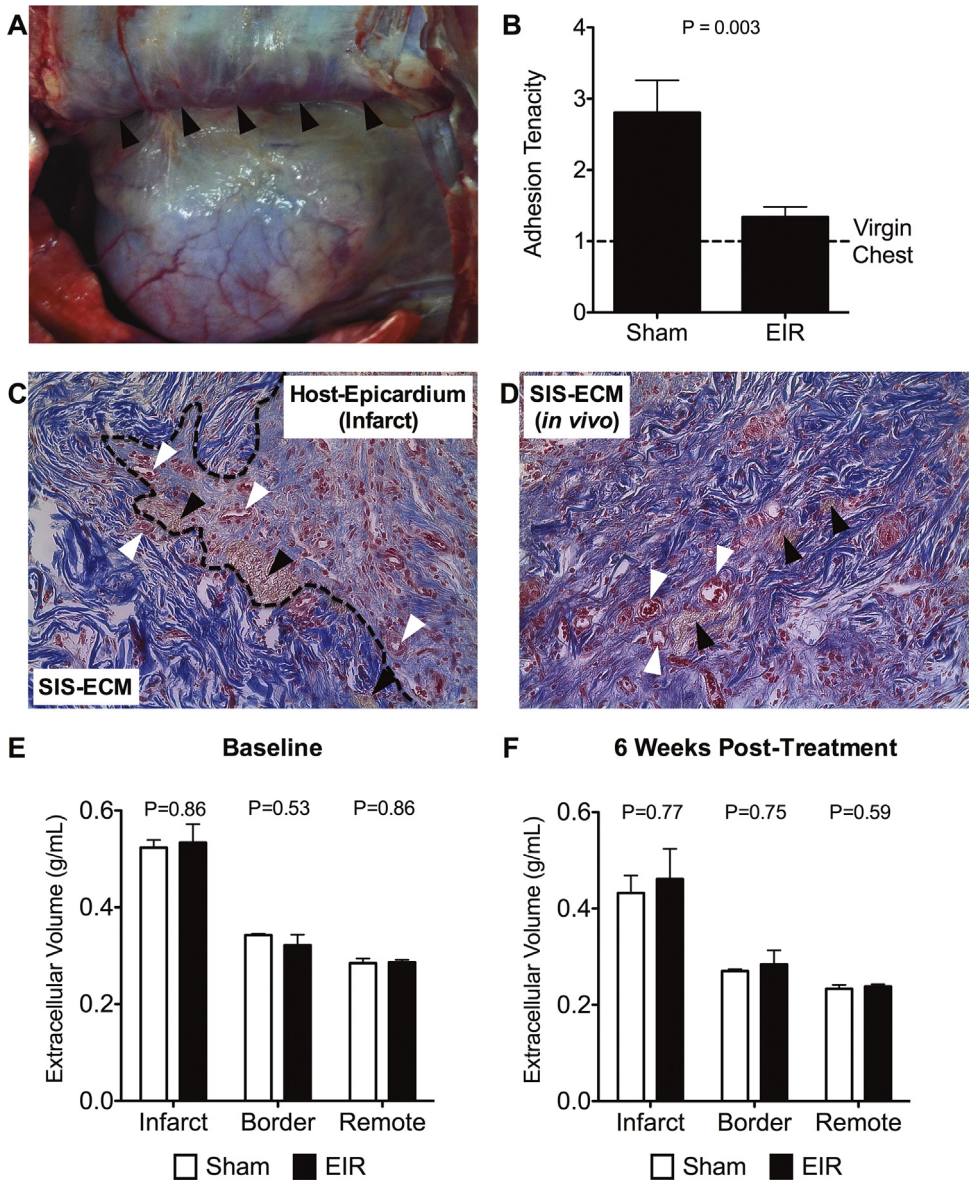

Figure 1 (A) Post-operative adhesions between the pericardium and sternum (arrowheads indicate adhesions). (B) Adhesion tenacity in epicardial infarct repair (EIR)–treated ($n = 8$) and sham-treated ($n = 4$) animals (1.3 ± 0.4 vs 2.8 ± 0.9, $p = 0.003$). Adhesion tenacity in a normal pig that did not undergo sternotomy is represented by the dashed line. (C and D) Histology stained with Masson's trichrome depicting the small intestine submucosa-extracellular matrix (SIS-ECM)–host-epicardium interface demonstrating integration of SIS-ECM with the epicardial surface (dashed line), granulation tissue formation (de novo collagen; black arrowheads), and small vascular structures (white arrowheads) around the SIS-ECM–host-epicardium interface (C) and within the SIS-ECM biomaterial (D). (E and F) Extracellular volume measured by CMR in EIR-treated and sham-treated animals within the infarct, border, and remote territories at baseline (infarct, 0.30 ± 0.02 g/ml vs 0.30 ± 0.02 g/ml, $p = 0.92$; border, 0.27 ± 0.01 g/ml vs 0.27 ± 0.01 g/ml, $p = 0.93$; remote, 0.29 ± 0.02 g/ml vs 0.30 ± 0.04 g/ml, $p = 0.81$) (E) and 6 weeks post-treatment (infarct, 0.24 ± 0.02 g/ml vs 0.24 ± 0.02 g/ml, $p = 0.96$; border, 0.23 ± 0.01 g/ml vs 0.24 ± 0.03 g/ml, $p = 0.48$; remote, 0.24 ± 0.01 g/ml vs 0.24 ± 0.01 g/ml, $p = 0.80$) (F).

Table 1 Semi-Quantitative Score System Used to Evaluate Post-Mortem Intrathoracic Adhesions

Adhesion tenacity score	0	1	2	3	4
Qualitative description of adhesion tenacity	No dissection[a]	Blunt dissection only	Blunt < sharp dissection	Blunt = sharp dissection	Blunt < sharp dissection

[a]Indicates the extent of dissection required to take down adhesions during heart explantation.

Statistical analysis

All data summaries are expressed as mean ± SD. GraphPad Prism 5.0 (GraphPad Software, Inc., La Jolla, CA) statistical software was used for all statistical analyses. The 2 groups were compared using the 2-sample *t*-test with unequal variances. Statistical significance was declared at 2-sided 5% α level. No adjustments for multiple testing were made. All statistical analyses were reviewed and confirmed by a biostatistician.

Results

Study animals

There were 12 animals randomly assigned to either sham ($n = 4$) or EIR (n = 8) groups. Animals were monitored daily for signs of heart failure, respiratory complications, infection, and sudden death, none of which were observed in either group.

Intrathoracic adhesions

Intrathoracic adhesions were assessed post-mortem in all animals to evaluate the impact of the implanted biomaterial on mediastinal fibrosis. Adhesion tenacity above that equivalent to a "virgin chest" was observed in all post-operative animals; however, in animals that received EIR, the tissue planes were more clearly defined and easily dissected, reflected by a lower adhesion tenacity score compared with animals that received sham treatment (1.3 ± 0.4 vs 2.8 ± 0.9, $p = 0.003$) (Figure 1B). Post-mortem examination revealed good integration of the SIS-ECM biomaterial without evidence of encapsulation. Integration with host myocardium was confirmed by histology, which demonstrated ingrowth of the epicardium into the SIS-ECM (Figure 1C) and infiltration of cells as well as the development of granulation tissue and vascular structures within the SIS-ECM (Figure 1C and D).

Interstitial myocardial fibrosis

ECV was assessed by CMR as a measure of myocardial fibrosis. Baseline CMR revealed an increase in ECV in infarcted vs normal animals (0.31 ± 0.02 g/ml vs 0.24 ± 0.01 g/ml, $p = 0.003$). Despite the addition of exogenous ECM in the animals receiving EIR, ECV within the infarcted territory was comparable in EIR-treated and sham-treated animals at baseline (0.53 ± 0.09 g/ml vs 0.52 ± 0.03 g/ml, $p = 0.86$) (Figure 1E). Although ECV decreased within all territories (infarct, peri-infarct, and remote myocardium) from baseline to 6 weeks, no difference was observed between EIR-treated and sham-treated animals (Figure 1E and F), indicating that the SIS-ECM biomaterial did not precipitate myocardial fibrosis.

Myocardial strain

Global myocardial restraint was assessed by passive pressure distention demonstrating no difference in left ventricular (LV) compliance between EIR-treated and sham-treated animals measured by LV volumes at various physiologic pressures (5 mm Hg, 31.07 ± 3.30 ml vs 33.40 ± 17.44 ml, $p = 0.83$; 10 mm Hg, 74.03 ± 15.10 ml vs 76.69 ± 32.20 ml, $p = 0.90$; 15 mm Hg, 117.0 ± 27.6 vs 120.0 ± 49.6 ml, $p = 0.93$) (Figure 2A), suggesting that SIS-ECM biomaterial applied to the epicardium does not adversely alter LV compliance and therefore should not impair LV filling.

Regional myocardial restraint was also assessed at the epicardial surface underlying the SIS-ECM biomaterial by measuring myocardial strain using CMR. At baseline, sham-treated animals demonstrate a positive strain (0.71 ± 1.36%) indicating dyskinesis in the infarcted myocardium, whereas EIR-treated animals demonstrate a neutral strain (−0.09 ± 2.04%), suggesting SIS-ECM may limit dyskinesis of the infarcted myocardium. By 6 weeks, strain in sham-treated animals became more positive (1.56 ± 2.03%, $p = 0.58$), consistent with worsening dyskinesis. However, in EIR-treated animals, strain became increasingly negative from baseline to 6 weeks (−0.09 ± 2.04% vs −2.29 ± 1.30%, $p = 0.049$) (Figure 2B), consistent with improved myocardial contraction suggestive of functional recovery.

Regional myocardial recovery

Measures of global LV function (Table 2) were similar between groups; however, significant regional changes within the infarcted myocardium were observed. Wall thickening measured by CMR demonstrated severe hypokinesis within the infarcted myocardium of EIR-treated and sham-treated animals at baseline (6.1 ± 7.9% vs 5.7 ± 6.7%, $p = 0.93$) (Figure 2C). A clinically significant increase in wall thickening demonstrating functional recovery was observed in EIR-treated animals compared with sham-treated animals by 6 weeks (28.6 ± 14.0% vs 4.2 ± 13.5%, $p = 0.021$) (Figure 2C and D). This functional improvement is observed in myocardial segments identified by CMR as non-viable despite successful revascularization, illustrating efficacy of therapy beyond the benefits of complete reperfusion.

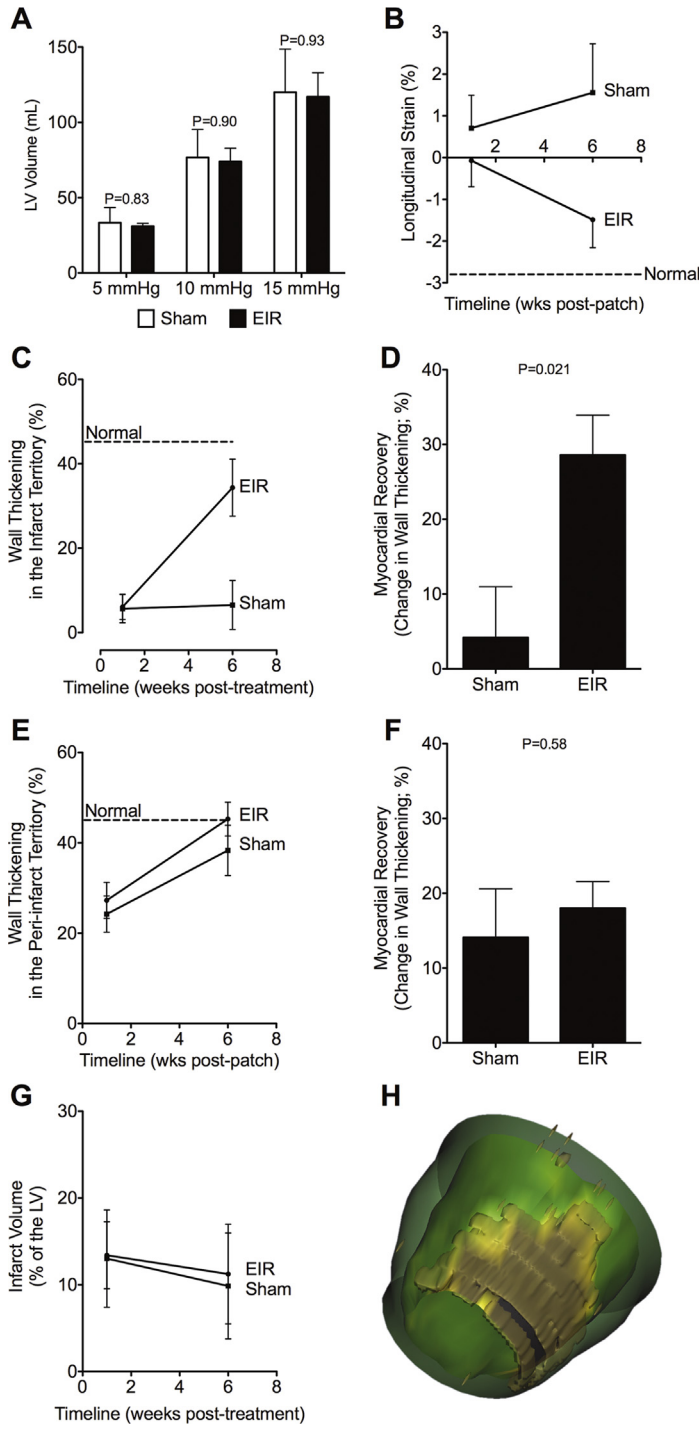

Figure 2 (A) LV volumes measured by passive pressure distention in epicardial infarct repair (EIR)–treated and sham-treated animals at 5 mm Hg (31.07 ± 3.30 ml vs 33.40 ± 17.44 ml, $p = 0.83$), 10 mm Hg (74.03 ml ± 15.10 vs 76.69 ± 32.20 ml, $p = 0.90$), and 15 mm Hg (117.0 ± 27.6 ml vs 120.0 ± 49.6 ml, $p = 0.93$). (B) Peak systolic longitudinal strain within the infarct territory from baseline to 6 weeks in EIR-treated animals (−0.09 ± 2.04% vs −2.29 ± 1.30%, $p = 0.049$) and sham-treated animals (0.71 ± 1.36% vs 1.56 ± 2.03%, $p = 0.58$). (C) Wall thickening (%) measured by CMR within the infarct territory of EIR-treated and sham-treated animals at baseline (6.09 ± 7.94% vs 5.67 ± 6.66%, $p = 0.93$) and 6 weeks (34.35 ± 17.85% vs 6.54 ± 11.59%, $p = 0.022$) after treatment. (D) Myocardial recovery within the infarct territory measured by the change in wall thickening (%) from baseline to 6 weeks after treatment in EIR-treated and sham-treated animals (28.62 ± 14.04% vs 4.21 ± 13.54%, $p = 0.021$). (E) Wall thickening (%) within the peri-infarct territory of EIR-treated and sham-treated animals at baseline (27.25 ± 11.29% vs 24.23 ± 8.01%, $p = 0.65$) and 6 weeks (45.27 ± 10.62% vs 38.33 ± 11.12%, $p = 0.32$) after treatment. (F) Myocardial recovery within the peri-infarct territory from baseline to 6 weeks after treatment in EIR-treated and sham-treated animals (18.02 ± 10.05% vs 14.11 ± 12.99%, $p = 0.58$). (G) Infarct volume (% of the LV) measured by LGE in EIR-treated and sham-treated animals at baseline (13.40 ± 3.85% vs 13.01 ± 5.61% of the LV) and 6 weeks (11.23 ± 5.74% vs 9.86 ± 6.12% of the LV) after treatment. (H) Three-dimensional reconstruction of the left ventricle depicting the infarct territory (yellow/gray) within the anterior LV wall.

Table 2 Measures of Global Left Ventricular Structure and Function in EIR-Treated and Sham-Treated Animals

	Sham (mean ± SD)	EIR (mean ± SD)	*p*-value
Baseline ejection fraction (%)	40.0 ± 5.8	41.5 ± 5.3	0.67
Ejection fraction (%) at 6 weeks	47.0 ± 7.2	50.8 ± 3.6	0.27
End-diastolic volume (ml) at 6 weeks	105.8 ± 13.3	96.6 ± 14.3	0.32
End-diastolic volume index[a] (ml/kg) at 6 weeks	2.01 ± 0.20	1.91 ± 0.22	0.44
End-systolic volume (ml) at 6 weeks	53.6 ± 15.0	47.6 ± 8.1	0.39
End-systolic volume index[a] (ml/kg) at 6 weeks	1.02 ± 0.25	0.94 ± 0.15	0.52

EIR, epicardial infarct repair.
[a]End-diastolic/end-systolic volume index = end-diastolic/end-systolic volume (ml) divided by animal weight (kg).

An improvement in wall thickening in the peri-infarct territory was also observed from baseline to 6 weeks after treatment in EIR-treated and sham-treated animals (18.0 ± 10.1% vs 14.1 ± 13.0%, $p = 0.58$); however, no significant difference in the magnitude of myocardial recovery was observed between groups (Figure 2E and F), suggesting that EIR had minimal influence beyond the effects of reperfusion on functional recovery within the border zone surrounding the infarct; myocardium likely to recover with successful reperfusion alone.

Infarct volume

Infarct volume was measured as a percent of the left ventricle by LGE on CMR. Infarct volume measured at baseline was not significantly different between EIR-treated and sham-treated animals (13.40 ± 3.85% vs 13.01 ± 5.61%, $p = 0.89$), indicating that the functional recovery observed in EIR-treated animals was not due to a smaller baseline infarct size. Infarct volume did not change significantly between baseline and 6 weeks in either EIR-treated or sham-treated animals (Figure 2G and H), suggesting the mechanism responsible for the functional recovery observed is not related to decreased infarct size.

Vasculogenesis and epicardial activation

Histologic examination of the explanted LV myocardium demonstrated regions of intact cardiomyocytes within the infarct (Figure 3A and B). Surrounding these regions was a marked increase in vascularity in EIR-treated animals vs sham animals (18.6 ± 5.6 vessels vs 4.8 ± 3.6 vessels per high-power field, $p = 0.004$) (Figure 3A–D). An increased density of small capillary vessels and small arteriolar vessels containing vascular smooth muscle cells was observed in EIR-treated animals vs sham-treated animals (9.8 ± 4.1 capillary vessels vs 3.8 ± 3.0 capillary vessels per high-power field, $p = 0.043$; 8.8 ± 1.9 arterioles vs 1.0 ± 0.8 arterioles per high-power field, $p < 0.0001$) (Figure 3E and F), suggesting EIR promotes vasculogenesis and may restore microvascular blood flow to these intact cardiomyocytes resulting in recovery of function in these otherwise likely hibernating cells.

Further histologic examination of the myocardium demonstrated an increase in vascularity within the epicardium underlying the SIS-ECM biomaterial (Figure 3C) and thickening of the epicardial surface in EIR-treated animals. Although the epicardial surface did appear activated in the sham-treated animals, the extent of epicardial thickening in the EIR-treated animals was significantly higher (3.8- ± 2.2-fold vs 7.9- ± 3.2-fold above normal; $p < 0.0001$) (Figure 4), suggesting that the increase in vascularity observed in EIR-treated animals may be the result of enhanced activation of the epicardium, perhaps involving EMT.

Discussion

ECM has been identified as a key player in myocardial healing after ischemic injury and an essential mediator for endogenous tissue repair and cell regeneration.[3,4,11] A biosurgical approach applying a healthy ECM construct, such as SIS-ECM, to the epicardial space after ischemic injury may promote endogenous repair. SIS-ECM is an ideal biomaterial for EIR given its commercial availability (approved by the US Food and Drug Administration for cardiac repair), biocompatibility, and established safety profile.[5–7] SIS-ECM has been used surgically for various intracardiac repairs.[8–17]

Pre-clinical safety

We assessed the safety of SIS-ECM applied to the epicardial surface after MI using a pre-clinical animal model by examining myocardial fibrosis, intrathoracic adhesion formation, and LV compliance. We show EIR does not increase myocardial fibrosis, despite the addition of exogenous ECM. We further demonstrate that post-operative adhesions are reduced in animals receiving EIR compared with animals receiving sham treatment, suggesting that SIS-ECM limits post-operative scar formation. This reduced scar formation may reduce the surgical difficulty associated with sternal re-entry. Although other groups observed immune or fibrotic reactions in response to the implantation of SIS-ECM in an intracardiac circumstance in children,[12] we show that SIS-ECM implanted onto the epicardial surface of the heart does not elicit a fibrotic response, suggesting that effects of SIS-ECM may depend on the location of implantation or the age of the recipient.

LV compliance was assessed by ex vivo passive pressure distention, the gold standard for assessment of global LV stiffness,[29] to ensure that the addition of non-compliant SIS-ECM biomaterial did not impede LV filling. EIR did not adversely alter global LV compliance and therefore should not negatively impact LV filling. We also measured

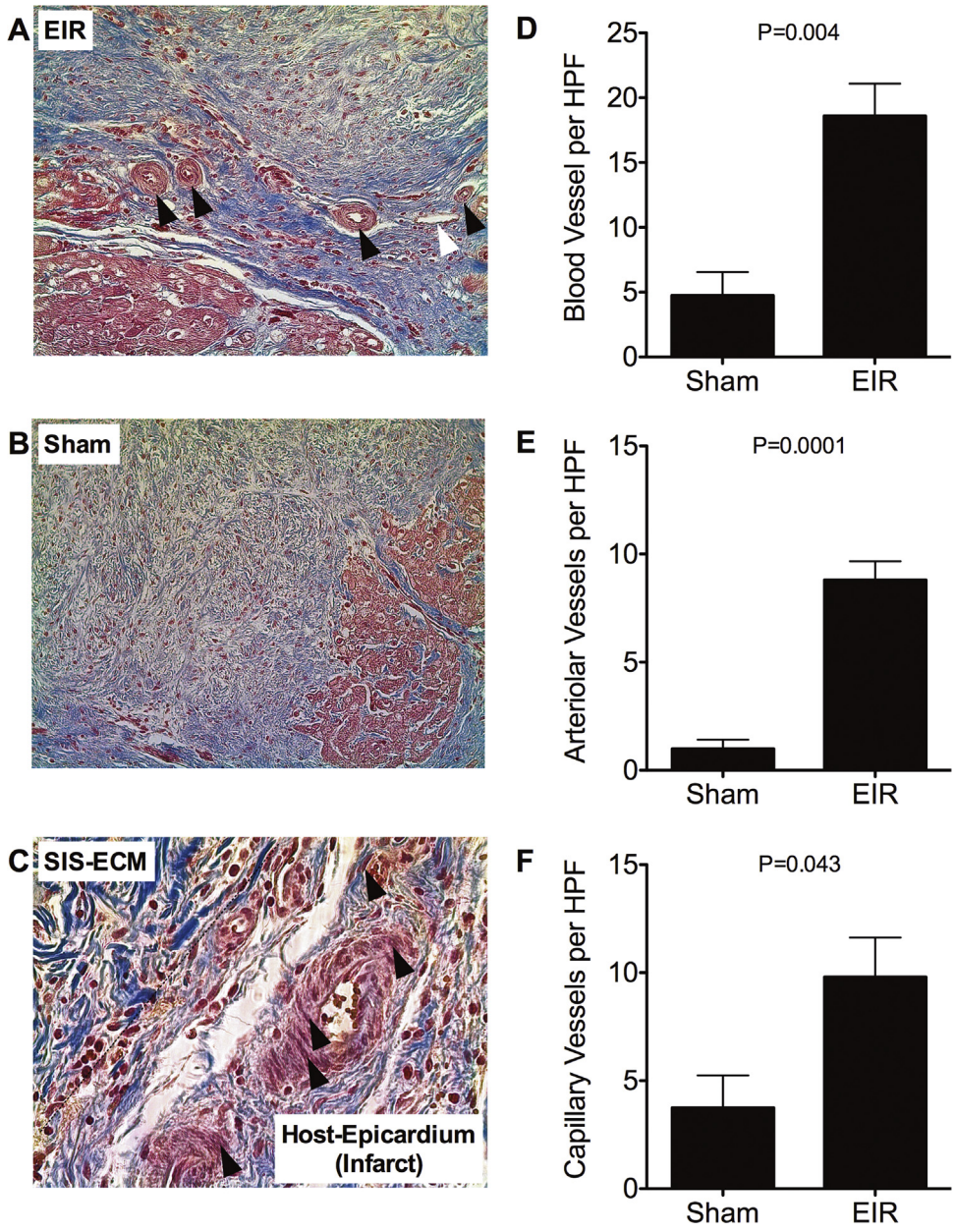

Figure 3 (A and B) Masson's trichrome staining of the infarcted myocardium of an epicardial infarct repair (EIR)–treated (A) and sham-treated (B) animal depicting islands of myocardial cells within the infarct scar and increased vascularity in EIR-treated animals (black arrowheads depict small arterioles; white arrowheads depict capillaries). (C) Masson's trichrome staining of the small intestine submucosa-extracellular matrix (SIS-ECM)–host-epicardium interface demonstrating arterioles containing vascular smooth muscle cells adjacent to the SIS-ECM biomaterial. Blood vessels (D), arteriolar vessels (E), and capillary vessels (F) per high-power field (HPF) within the infarcted myocardium of EIR-treated ($n = 4$) and sham-treated ($n = 4$) animals (blood vessels, 18.6 ± 5.6 vs 4.8 ± 3.6, $p = 0.004$; arterioles, 8.8 ± 1.9 vs 1.0 ± 0.8, $p = 0.0001$; capillaries, 9.8 ± 4.1 vs 3.8 ± 3.0, $p = 0.043$).

myocardial strain by CMR to assess the regional effects of SIS-ECM on myocardial restraint. Morita et al[23] previously correlated changes in longitudinal strain patterns in the anterior wall after MI with response to other infarct-limiting therapies. We measured peak systolic longitudinal strain referenced to the end-diastolic epicardial surface. Negative strain reflects shortening of the LV myocardium during systole, which is expected to occur in healthy functional myocardium. Positive strain reflects lengthening of the LV myocardium indicating dyskinesis. We observed a trend toward dyskinesis in animals receiving sham treatment; however, in animals receiving EIR, a neutral strain was observed at baseline, indicating that the SIS-ECM biomaterial may be restraining paradoxical myocardial tissue deformation, preventing dyskinesis. Together, these data demonstrate that EIR limits dyskinesis without adversely altering LV compliance.

EIR enhances functional myocardial recovery after MI

In a rodent model of MI, we previously demonstrated that EIR attenuates LV dilation and improves LV contractility,

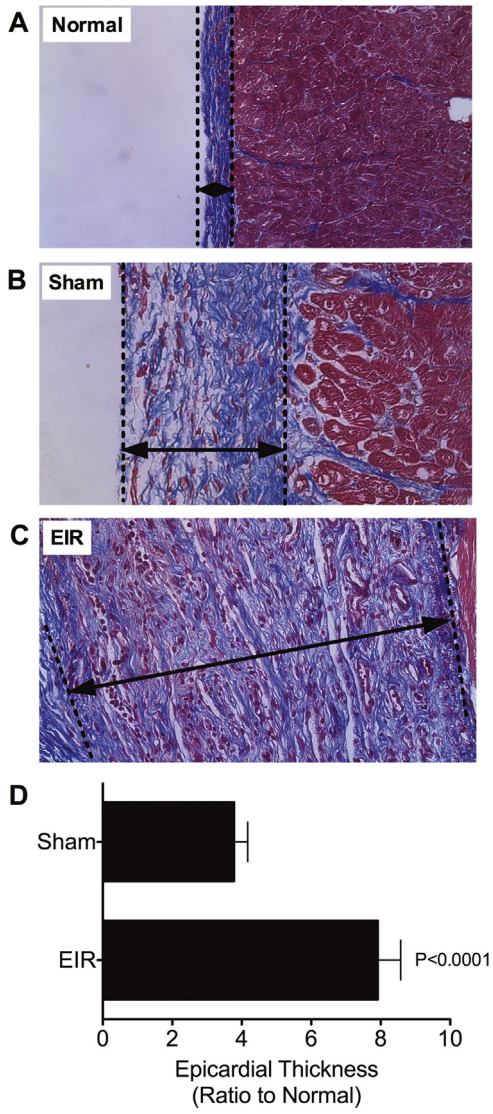

Figure 4 (A–C) Masson's trichrome staining of the epicardium overlying the infarcted myocardium of a representative normal (A), sham-treated (B), and epicardial infarct repair (EIR)–treated (C) animal depicting epicardial thickness (distance between the dashed lines represented by the arrow). (D) Epicardial thickness of sham-treated ($n = 4$; 3.78- ± 2.21-fold above normal) and EIR-treated ($n = 4$; 7.92- ± 3.23-fold above normal) animals measured as a ratio to the epicardial thickness of normal animals ($n = 4$; $p < 0.0001$).

resulting in a clinically significant increase in ejection fraction.[8] Given the small size of the rodent heart, this model lacked the spatial resolution to determine whether EIR positively influences global LV function by promoting recovery of the infarcted myocardium or enhancing compensation by the remote myocardium. In this study, we adapted a larger pre-clinical porcine model to examine the regional effects of EIR on the infarct, peri-infarct, and remote myocardial territories. Ischemia-reperfusion of the diagonal coronary arteries produced a discrete MI ideal for regional analysis. Global LV function was not significantly affected; however, an improvement in regional wall thickening was observed in animals that received EIR, demonstrating that EIR improves contractility by promoting functional recovery of the infarcted myocardium.

We also show that EIR promotes functional recovery of the infarcted myocardium beyond that achieved by reperfusion alone. Kim et al[25] previously showed that after MI, <10% of myocardial segments with >50% LGE by CMR demonstrate functional improvement in response to complete revascularization, establishing >50% LGE as the threshold for predicting myocardial viability for surgical revascularization. Similarly, in our ischemia-reperfusion model, we observed no significant improvement in function within the infarcted myocardium of animals receiving sham treatment. However, a significant improvement in myocardial function was observed within the infarcted myocardium of animals receiving EIR. This improvement demonstrates that EIR promotes functional recovery of the infarcted myocardium previously thought to be non-viable when treated by conventional revascularization alone.

Putative mechanisms of benefit

Infarct size was neither variable between groups nor significantly altered over time in either group, suggesting that the functional recovery observed was unrelated to infarct size. Significant changes in markers of improved myocardial healing were observed, including epicardial activation and vasculogenesis. Epicardial thickening in response to ischemic injury has been shown to act as a source of paracrine factors, including the angiogenic factors fibroblast growth factor-2 and vascular endothelial growth factor, which condition the underlying myocardium for repair.[18] Epicardial thickening was enhanced by EIR. Furthermore, numerous key stem cell niches are located within the epicardium.[19,20] Activation and mobilization of these stem cell populations through EMT is believed to occur in response to ischemic injury and acts to stimulate myocardial repair (Figure 5).[21,22,30] Following EMT, these cells can differentiate into vascular smooth muscle cells and form new blood vessels (vasculogenesis) within the infarcted myocardium.[31,32] We show that EIR results in increased vascularity, particularly small arteriolar networks closely associated with islands of intact cardiomyocytes, within the infarcted myocardium (Figure 4A), suggesting that EIR may restore perfusion at a microvascular level to rescue otherwise hibernating myocardium. Recovery of function in this hibernating but intact myocardium may explain the improvement in function observed in the absence of altered infarct size, although further investigation of this putative mechanism is required.

Clinical perspective

A significant subset of patients admitted to the hospital for acute coronary syndromes undergo surgical revascularization early after MI.[33] These patients are at increased risk of incomplete revascularization, and the infarcted myocardium is not directly addressed at the time of CABG. These pre-clinical data suggest that when applied in addition to successful reperfusion, EIR may promote functional recovery in what was previously deemed non-viable myocardium.

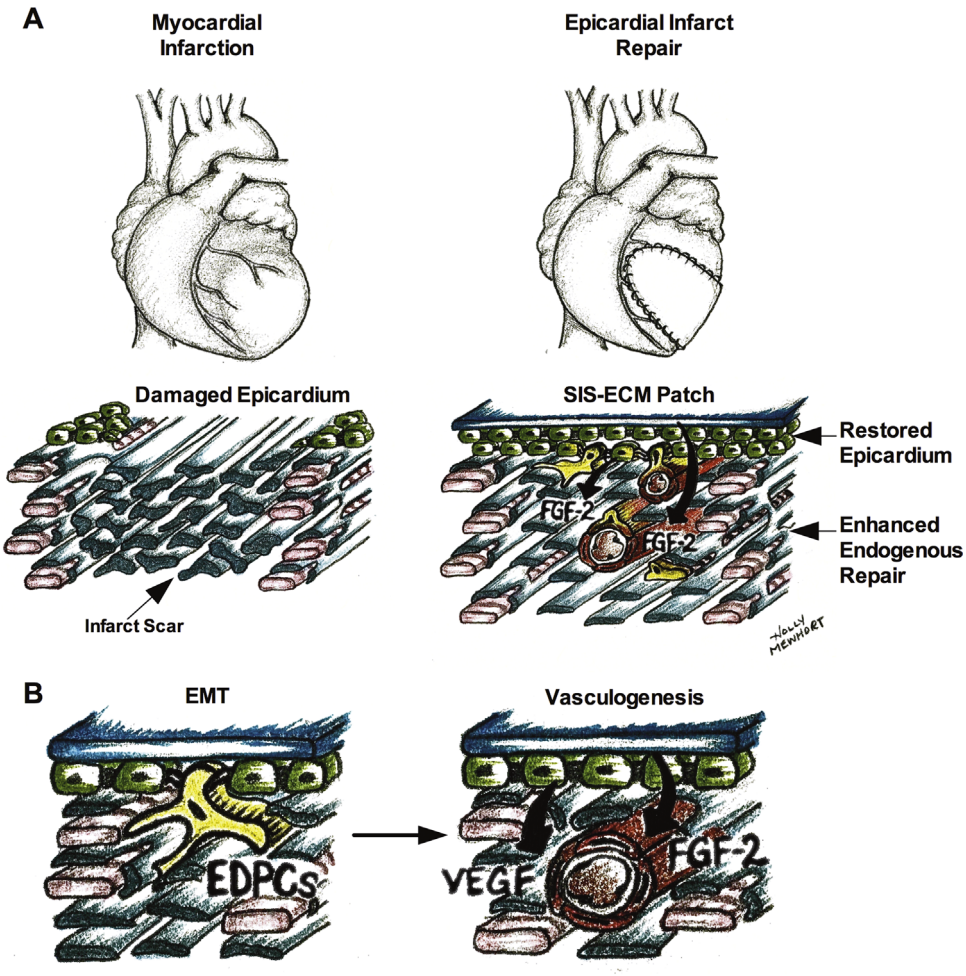

Figure 5 (A and B) Graphic representation of the proposed mechanism by which EIR promotes infarct healing, including activation of the epicardium (A), leading to mobilization of epithelium-derived progenitor cells (EDPCs) through epithelial mesenchymal transition (EMT) and differentiation of these cells into vascular smooth muscle cells under the influence of vascular endothelial growth factor (VEGF) and fibroblast growth factor-2 (FGF-2) released by the activated epicardium and present within the small intestine submucosa-extracellular matrix (SIS-ECM) biomaterial (B).

Limitations

Although we have yet to identify the optimal therapeutic window for EIR after MI, we hypothesize that the greatest benefits will be achieved early. We appreciate that our pre-clinical model is likely to portray the maximal benefits of EIR, as it was applied immediately after ischemic injury. Clinically, if performed as an adjunct to CABG, most patients will receive EIR during the sub-acute stage after MI. We previously demonstrated that EIR improves myocardial function when applied during the sub-acute to chronic stage after MI.[8] Although the optimal therapeutic window is currently under investigation, our findings suggest that patients undergoing CABG during the acute or sub-acute stages after MI may stand to benefit from adjunct EIR. However, given the small sample size of this study, further pre-clinical studies may be warranted before clinical translation.

In conclusion, EIR is safe and effective. EIR restores regional myocardial function beyond that which can be achieved by reperfusion alone.

Disclosure statement

None of the authors has a financial relationship with a commercial entity that has an interest in the subject of the presented manuscript or other conflicts of interest to disclose.

Funding was provided by Alberta Innovates Health Solutions (H.E.M.M), Heart and Stroke Foundation of Canada (P.W.M.F.), and CorMatrix Cardiovascular, Inc. (P.W.M.F.). CorMatrix Cardiovascular, Inc., contributed unrestricted research grant funding to this research but had no role in the study design, data collection, data analysis, manuscript compilation, or revision. CorMatrix Cardiovascular, Inc., has not read or approved this manuscript. No authors hold financial interest in CorMatrix Cardiovascular, Inc.

The authors thank the following individuals and facilities: Loreen Thon, RT, who performed CMR image acquisition; Amy Bromley, MD, FRCPC, who reviewed all histologic analyses; Brodie Lipon, BSc, and Daniel Park, BSc, who assisted with animal preparation and recovery; the Stephenson Cardiovascular MR Centre, where all CMR image acquisition and analysis were performed; the Libin Core Pathology Laboratory, which processed the histologic specimens; and the University of Calgary Animal Resource Centre, which housed all experimental animals.

References

1. Go AS, Mozaffarian D, Roger VL, et al. Executive summary: heart disease and stroke statistics—2013 update: a report from the American Heart Association. Circulation 2013;127:143-52.
2. Murphy-Ullrich JE. The de-adhesive activity of matricellular proteins: is intermediate cell adhesion an adaptive state? J Clin Invest 2001;107:785-90.
3. Bayomy AF, Bauer M, Qiu Y, Liao R. Regeneration in heart disease—is ECM the key? Life Sci 2012;91:823-7.
4. Mercer SE, Odelberg SJ, Simon H-G. A dynamic spatiotemporal extracellular matrix facilitates epicardial-mediated vertebrate heart regeneration. Dev Biol 2013;382:457-69.
5. Baicu CF, Stroud JD, Livesay VA, et al. Changes in extracellular collagen matrix alter myocardial systolic performance. Am J Physiol Heart Circ Physiol 2003;284:H122-32.
6. Badylak SF. Xenogeneic extracellular matrix as a scaffold for tissue reconstruction. Transpl Immunol 2004;12:367-77.
7. Daly KA, Stewart-Akers AM, Hara H, et al. Effect of the alphaGal epitope on the response to small intestinal submucosa extracellular matrix in a nonhuman primate model. Tissue Eng Part A 2009;15:3877-88.
8. Mewhort HEM, Turnbull JD, Meijndert HC, Ngu JMC, Fedak PWM. Epicardial infarct repair with basic fibroblast growth factor-enhanced CorMatrix-ECM biomaterial attenuates postischemic cardiac remodeling. J Thorac Cardiovasc Surg 2014;147:1650-9.
9. Witt RG, Raff G, Van Gundy J, Rodgers-Ohlau M, Si M-S. Short-term experience of porcine small intestinal submucosa patches in paediatric cardiovascular surgery. Eur J Cardiothorac Surg 2013;44:72-6.
10. Scholl FG, Boucek MM, Chan K-C, Valdes-Cruz L, Perryman R. Preliminary experience with cardiac reconstruction using decellularized porcine extracellular matrix scaffold: human applications in congenital heart disease. World J Pediatr Congenit Heart Surg 2010;1:132-6.
11. Ott HC, Matthiesen TS, Goh S-K, et al. Perfusion-decellularized matrix: using nature's platform to engineer a bioartificial heart. Nat Med 2008;14:213-21.
12. Zaidi AH, Nathan M, Emani S, et al. Preliminary experience with porcine intestinal submucosa (CorMatrix) for valve reconstruction in congenital heart disease: histologic evaluation of explanted valves. J Thorac Cardiovasc Surg 2014;148(2216-25):e1.
13. Fedak PWM. Cardiac progenitor cell sheet regenerates myocardium and renews hope for translation. Cardiovasc Res 2010;87:8-9.
14. Fedak PWM, Bai L, Turnbull J, Ngu J, Narine K, Duff HJ. Cell therapy limits myofibroblast differentiation and structural cardiac remodeling: basic fibroblast growth factor-mediated paracrine mechanism. Circ Heart Fail 2012;5:349-56.
15. Fedak PWM, Szmitko PE, Weisel RD, et al. Cell transplantation preserves matrix homeostasis: a novel paracrine mechanism. J Thorac Cardiovasc Surg 2005;130:1430-9.
16. Fazel S, Chen L, Weisel RD, et al. Cell transplantation preserves cardiac function after infarction by infarct stabilization: augmentation by stem cell factor. J Thorac Cardiovasc Surg 2005;130:1310.
17. Badylak S, Freytes D, Gilbert T. Extracellular matrix as a biological scaffold material: structure and function. Acta Biomater 2009;5:1-13.
18. Zhou B, Honor LB, He H, et al. Adult mouse epicardium modulates myocardial injury by secreting paracrine factors. J Clin Invest 2011;121:1894-904.
19. Smart N, Riley PR. The epicardium as a candidate for heart regeneration. Future Cardiol 2012;8:53-69.
20. Smart N, Bollini S, Dubé KN, et al. De novo cardiomyocytes from within the activated adult heart after injury. Nature 2011;474:640-4.
21. van Wijk B, Gunst QD, Moorman AFM, van den Hoff MJB. Cardiac regeneration from activated epicardium. PLoS One 2012;7:e44692.
22. Balmer GM, Bollini S, Dubé KN, Martinez-Barbera JP, Williams O, Riley PR. Dynamic haematopoietic cell contribution to the developing and adult epicardium. Nat Commun 2014;5:4054.
23. Morita M, Eckert CE, Matsuzaki K, et al. Modification of infarct material properties limits adverse ventricular remodeling. Ann Thorac Surg 2011;92:617-24.
24. Chow K, Flewitt JA, Green JD, Pagano JJ, Friedrich MG, Thompson RB. Saturation recovery single-shot acquisition (SASHA) for myocardial T1 mapping. Magn Reson Med 2014;71:2082-95.
25. Kim RJ, Wu E, Rafael A, et al. The use of contrast-enhanced magnetic resonance imaging to identify reversible myocardial dysfunction. N Engl J Med 2000;343:1445-53.
26. Satriano A, Rivolo S, Martufi G, Finol EA, Di Martino ES. In vivo strain assessment of the abdominal aortic aneurysm. J Biomech 2015;48:354-60.
27. Walther T, Schubert A, Falk V, et al. Left ventricular reverse remodeling after surgical therapy for aortic stenosis: correlation to renin-angiotensin system gene expression. Circulation 2002;106(12 Suppl 1):I23-6.
28. Konertz WF, Kostelka M, Mohr FW, et al. Reducing the incidence and severity of pericardial adhesions with a sprayable polymeric matrix. Ann Thorac Surg 2003;76:1270-4.
29. Burkhoff D. Assessment of systolic and diastolic ventricular properties via pressure-volume analysis: a guide for clinical, translational, and basic researchers. Am J Physiol Heart Circ Physiol 2005;289:H501-12.
30. Bock-Marquette I, Saxena A, White MD, Dimaio JM, Srivastava D. Thymosin beta4 activates integrin-linked kinase and promotes cardiac cell migration, survival and cardiac repair. Nature 2004;432:466-72.
31. Smart N, Risebro CA, Melville AAD, et al. Thymosin beta4 induces adult epicardial progenitor mobilization and neovascularization. Nature 2007;445:177-82.
32. Bock-Marquette I, Shrivastava S, Pipes GCT, et al. Thymosin beta4 mediated PKC activation is essential to initiate the embryonic coronary developmental program and epicardial progenitor cell activation in adult mice in vivo. J Mol Cell Cardiol 2009;46:728-38.
33. Wallentin L, Becker RC, Budaj A, et al. Ticagrelor versus clopidogrel in patients with acute coronary syndromes. N Engl J Med 2009;361:1045-57.